2017 International Nuclear Atlantic Conference - INAC 2017
Belo Horizonte, MG, Brazil, October 22-27, 2017
ASSOCIAÇÃO BRASILEIRA DE ENERGIA NUCLEAR - ABEN

Agência Brasileira do ISBN
ISBN 978-85-99141-07-6
9 788599 141076

TRANSIENT MODELLING OF A NATURAL CIRCULATION LOOP UNDER VARIABLE PRESSURE

André L. B. Vianna[1], José L. H. Faccini[2] and Jian Su[1]

[1]Programa de Engenharia Nuclear, COPPE
Universidade Federal do Rio de Janeiro
21941-972 Rio de Janeiro, RJ
avianna@nuclear.ufrj.br
sujian@nuclear.ufrj.br

[2]Laboratório de Termo-Hidráulica Experimental
Instituto de Engenharia Nuclear (IEN/CNEN)
R. Hélio de Almeida, 75, Cidade Universitária,
21941-906 Rio de Janeiro, RJ
faccini@ien.gov.br

ABSTRACT

The objective of the present work is to model the transient operation of a natural circulation loop, which is one-tenth scale in height to a typical Passive Residual Heat Removal system (PRHR) of an Advanced Pressurized Water Nuclear Reactor and was designed to meet the single and two-phase flow similarity criteria to it. The loop consists of a core barrel with electrically heated rods, upper and lower plena interconnected by hot and cold pipe legs to a seven-tube shell heat exchanger of countercurrent design, and an expansion tank with a descending tube. A long transient characterized the loop operation, during which a phenomenon of self-pressurization, without self-regulation of the pressure, was experimentally observed. This represented a unique situation, named natural circulation under variable pressure (NCVP). The self-pressurization was originated in the air trapped in the expansion tank and compressed by the loop water dilatation, as it heated up during each experiment. The mathematical model, initially oriented to the single-phase flow, included the heat capacity of the structure and employed a cubic polynomial approximation for the density, in the buoyancy term calculation. The heater was modelled taking into account the different heat capacities of the heating elements and the heater walls. The heat exchanger was modelled considering the coolant heating, during the heat exchanging process. The self-pressurization was modelled as an isentropic compression of a perfect gas. The whole model was computationally implemented via a set of finite difference equations. The corresponding computational algorithm of solution was of the explicit, marching type, as for the time discretization, in an upwind scheme, regarding the space discretization. The computational program was implemented in MATLAB. Several experiments were carried out in the natural circulation loop, having the coolant flow rate and the heating power as control parameters. The variables used in the comparison between experimental and calculated data were some relevant loop temperatures and pressures. The results obtained from the computational model agree qualitatively well with the experimental NCVP data.

1. INTRODUCTION

Natural circulation is the phenomenon of convection taking place in a closed circuit or loop, provided that there is a heat source in its lower portion and a heat sink in its upper portion, in the presence of gravity. In order to function, the natural circulation does not depend on any moving parts or mechanical devices, like pumps, so its associated reliability

is very high. For such reason, the passive residual heat removal (PRHR) systems of third-generation, advanced passive nuclear reactors, like the AP600 and AP1000 Westinghouse pressurized water reactor (PWR) designs, are natural circulation loops.
Even though they are reliable and safe, the natural circulation systems have, both in single and two-phase flow, the drawback of frequent instabilities, or oscillations when they occur in a repetitive manner. The instabilities have to be studied, as they can damage the systems with excessive vibrations, pressure or temperature variations and other problems.
The occurrence of instabilities in the natural circulation, including geysering, has been long studied, using both vertical columns [1] and single-channel natural circulation loops [2]. Although geysering is a two-phase flow oscillation, characterized by a violent vapor eruption, its most important feature is the long building-up process of heat accumulation in the heater, which takes place, basically, in single-phase flow [3]. This allows for reasonably good approximations via the utilization of relatively simple modelling.
It is possible to employ a set of finite difference equations in order to model, conveniently, the transient behavior of single-phase natural circulation in a single-channel loop [4]. In doing so, good approximation between calculated and experimental data may be achieved by assuming uniform flow rate throughout the loop, in the momentum equation, as well as constant coolant temperature, in the heat exchanger, regarding the energy equation, and the Boussinesq approximation, with the density calculated by a third-degree polynomial. The same loop and assumption above have been used for studying the transient, oscillatory behavior of the two-phase flow, also with good results [5].
On the other hand, the same assumptions above mentioned have been applied to the study of both steady-state and transient single-phase flow in a natural circulation system, but using a lumped parameter method [6]. A reasonable agreement between calculated and experimental data was obtained, with a maximum deviation of 30%.
PRHR systems, more specifically, have been subject to thermal hydraulic analysis [7]. Such a system, belonging to an integral PWR, was studied, again assuming uniform flow rate. Even though it was pointed out that, especially for two-phase flow, inaccuracy may arise from such simplification, the comparison between the results thus obtained and data got from RETRAN-02 and RELAP/MOD3 showed good agreement, with the conclusion the simplified model utilized was apt for the PRHR analysis.
Transients in a natural circulation loop, under typical PWR conditions and in the presence of non-condensable gas (NCG), have also been modelled [8]. Although it was concluded that the NCG was a source of uncertainty and discrepancies between calculated and experimental data, these showed, anyway, good agreement.
The role of the expansion tank in a single-phase natural circulation loop has been analysed [9]. It was observed that such loop component, in that case open to the atmosphere, played a very important role, as long as it accommodated the swells and shrinkages of the loop primary fluid during a transient, typically represented by a power increase.
The stability of a self-pressurized natural circulation integral reactor has been modelled [10]. A proper thermohydraulic model was developed, and the results obtained from it were compared to those originated in a simpler analytical model, with good agreement. In the model, the coolant pressure fluctuations were modelled with instantaneous feedback, in a process of immediate self-regulation of the pressure.
The objective of the present work is to model the transient operation of a natural circulation loop (NCL). The NCL is characterized not only by its construction, according to a one-tenth scale in height to the AP600 PRHR system, but also by its design, carried out to meet the single and two-phase flow similarity criteria to that system. For so, this

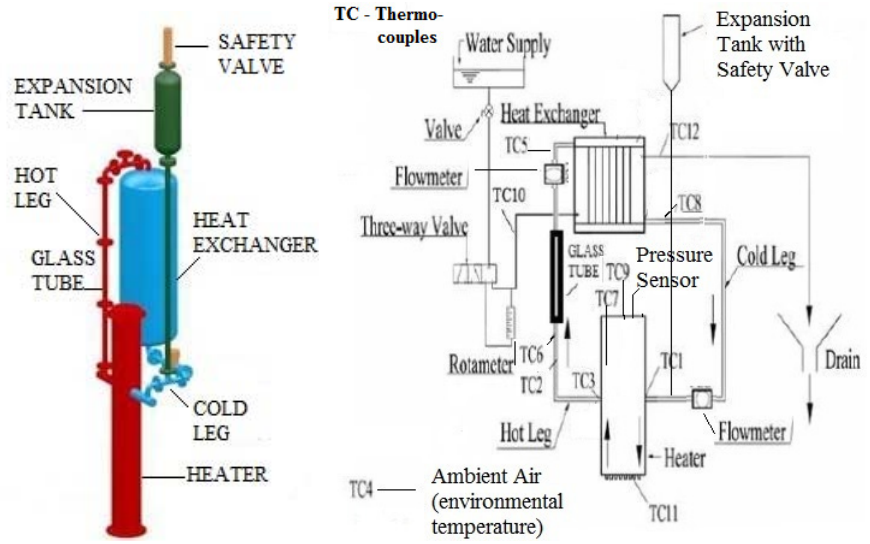

Figure 1: NCL main components (out of scale) and instrumentation.

work is divided into 5 sections. After this Introduction, the Experimental Apparatus is described. Next, the adopted Modelling is presented, with its physical and mathematical components. Then, the Results and Discussions section presents a comparison between experimental and calculated data and the corresponding analysis. The Conclusions summarize the work, list the main findings and indicate the future research correlated.

2. EXPERIMENTAL APPARATUS

The loop studied in the present work was the Nuclear Engineering Institute Natural Circulation Loop, named NCL. The NCL was designed in order to meet the single and two-phase flow similarity criteria to the PRHR system of an advanced PWR, in a 1:10 scale in height, with 0.94 m between the middle points of the heated section, in the heater, and the heat exchanger (HX), as well as external diameters of 0.19 m for the heater and 0.28 m for the HX. See Fig. 1 for the NCL main components and instrumentation. The core barrel heater was composed by 52 cartridge resistance rods, equally spaced in a square array, electrically heated with up to 30 W each. The heated section length was 0.366 m, between the heights of 0.136 m and 0.502 m from the lowest point of the heater. Upper and lower plena linked the heater to the HX, via hot and cold pipe legs, respectively, internal diameter 0.0234 m. The NCL was thermally insulated with rock wool.
The HX, of the shell and tube type, was composed by 7 tubes, equally spaced in a triangular array, each one 0.6 m long, wall thickness 0.001 m. The design was countercurrent. Primary water flowed down inside the tubes and the secondary, coolant water flowed up between the tubes with an average initial temperature of 25 °C. The coolant flow rate was controlled, via a rotameter. The NCL experiments were performed with a step power increase to a fixed value, as well as a constant coolant flow rate, according to one of the following values: 3 l/h, 6 l/h, 9 l/h or 12 l/h. Such power and coolant flow rate functioned as the control parameters for the several NCL experiments carried out.
The expansion tank was located in the upmost part of the NCL, thus pressurizing the NCL, as long as it was not open to the atmosphere, but closed instead, with a safety valve (opening pressure 34.335 kPa) mounted on its top. The expansion tank was cylindrically

shaped, external diameter 0.21 m and height 0.395 m. Before an experiment, when the NCL was filled with water, the expansion tank was left with air in its top part, occupying an average value of two thirds of the total expansion tank volume. This was for accommodating the primary water dilatation, due to the experimental heating. A descending tube, length 1.2 m, linked the tank to the loop, in the cold leg, close to the heater.
Monitoring, as well as data processing and control systems were provided to the NCL. Those included power, flow rate, pressure and temperature data storage, employing a PXI industrial computer and the LabVIEW software. See [11] for the detailed positioning, in the NCL, of its 12 type K thermocouples.
In Fig. 1, the hot and cold leg flowmeters were of the Doppler type. The pressure sensor measured the absolute pressure inside the heater, below the heater upper cover. The glass tube allowed for the hot leg flow visualization and recording, as well as image capturing, by means of a high-speed digital camera. It was equipped with zoom lenses, among other devices, like proper light projectors, an image acquisition program and a dedicated PC.

3. MODELLING

3.1. Physical Model

This work presents a modelling of the transient operation of a natural circulation loop. The transient was represented by a step power increase, with different cooling conditions. Fig. 2 represents the physical model adopted for the NCL. It was assumed turbulent and laminar flow regime for the primary and secondary fluids, respectively. The turbulent flow was modelled in accordance with the Dittus-Boelter correlation, following [12]. As for the laminar flow, appropriate Nusselt numbers were employed, both for tubes (in the case of the heat exchange between the coolant and the HX walls) and for a tube array (in the case of the heat exchange between the coolant and the HX tubes).
The NCL physical model took into account the whole thermal capacity of the structure. A polynomial of the third degree was used in the primary density calculation. The heater was modelled considering the different thermal capacities of the heating elements (cartridge resistances) and the heater walls. The HX was modelled accounting for the coolant heating during the heat exchange with the primary fluid.
As above mentioned, the primary fluid, when dilating during each NCL experiment, compressed the expansion tank air. Such air was trapped there because the loop was filled with water from the bottom, using a centrifugal pump. That process was modelled as the isentropic compression of a perfect gas (air).
In the loop resistance calculation, it was included a form loss term, as shown in [12], in addition to the friction term, solely employed by [4]. The friction and the form loss terms were calculated for the main NCL components, namely the heater, heat exchanger, hot leg and cold leg. In the friction terms, the relation by Creveling *et al.* for closed loops, mentioned by [13], was employed. The form loss terms were calculated according to [12].

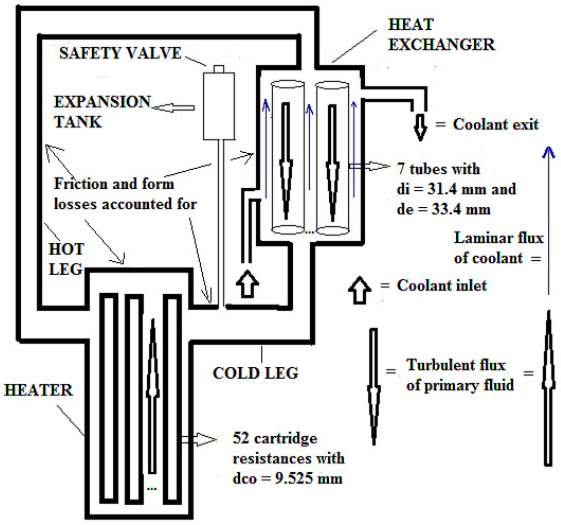

Figure 2: NCL physical model.

3.2. Mathematical Model

3.2.1. Conservation equations and constitutive relation

Initially oriented to the single-phase flow, the mathematical transient modelling employed in this paper follows, in general, the treatment of [4]. However, new characteristics were introduced in the model, as a function of the NCL specificities mentioned above. These are the different thermal capacities of the heater components; the coolant heating inside the HX; the isentropic air compression inside the expansion tank; and the addition of the form loss term to the friction term, in the total loop resistance calculation.
The mass, energy and momentum conservation equations are employed, in order to model the long single-phase transient, which characterizes the NCL operation, until the first geysering eruption takes place. See [11] for a detailed explanation about the geysering occurrence in the NCL. In the model, one-dimensional flow through a channel of constant area is assumed, thus following the treatment of loop flows by [13]:

$$\frac{\partial \rho}{\partial t} + \frac{\partial G}{\partial x} = 0 \tag{1}$$

$$\frac{\partial(\rho h - p)}{\partial t} + \frac{\partial(Gh)}{\partial x} - u\frac{\partial p}{\partial x} = q''' + \frac{ufG|G|}{2D_e\rho} \tag{2}$$

$$\frac{\partial(\rho u)}{\partial t} + \frac{\partial(Gu)}{\partial x} = -\frac{\partial p}{\partial x} - \rho g cos\theta - \frac{fG|G|}{2D_e\rho} \tag{3}$$

where t is the time, G is the mass flux, x is the flow coordinate, and ρ is the fluid density. Eq. (1) is the mass conservation equation.
As for the energy conservation equation, its initial form is given by Eq. (2), where h is the enthalpy, p is the pressure, u is the flow velocity, q''' is the volumetric heat-generation rate, f is the friction factor and D_e is the equivalent diameter of the cross section.
Regarding the momentum conservation equation, its initial form is given by Eq. (3), where g is the gravity acceleration. The angle between the vertical and the flow directions is θ. Now, Eq. (1) is used in order to simplify Eq. (2), in which single-phase flow is assumed.

Also, the friction and the pressure variations are neglected. In this way, Eq. (4) arises, where the primary fluid properties are the specific heat C_p and the temperature T. The linear heat-generation rate is q' and the loop cross section area is A.

$$\rho C_p A \left(\frac{\partial T}{\partial t} + u \frac{\partial T}{\partial x} \right) = q' \tag{4}$$

$$q' = -UP(T - T_c) \tag{5}$$

The term q', defined above for the heater, is zero in the loop tubes. In the HX, it is defined by Eq. (5), where U is the global heat transfer coefficient, P is the perimeter of heat exchanging and T_c is the coolant temperature.
The heat transfer between the fluid and the loop structure is modelled via a thermal balance for the latter, according to Eq. (6). The subscript w refers to the structure (wall). In this way, H_w is the heat transfer coefficient between the fluid and the structure; and the wall thickness of the structure is δ_{w}.

$$\rho_w C_{pw} \delta_w \frac{dT_w}{dt} = H_w \left(T - T_w \right) \tag{6}$$

$$\rho C_p A \left(\frac{\partial T}{\partial t} + u \frac{\partial T}{\partial x} \right) = q' - H_w P_w (T - T_w) \tag{7}$$

Considering the heat transfer for the structure, Eq. (4) is rewritten as Eq. (7).

$$-\int \rho g cos\theta dx = -\int \rho_h g cos\theta dx - \int \rho_c g cos\theta dx = (\rho_c - \rho_h) g (Z_{max} - Z_{min}) = \Delta P_b \tag{8}$$

$$-\int \frac{fG|G|}{2D_e \rho} dx = -\Delta P f \tag{9}$$

Now, Eq. (1) is used for simplifying Eq. (3), which has each term integrated around the loop. The first right term drops, as there is no pump in a natural circulation loop. Then, a notation similar to the employed by [13] is used, so the buoyancy term, which drives the natural circulation in the loop, is represented, in Eq. (8), by ΔP_b. The subscripts h and c refer to the hot and cold legs, and the maximum and minimum loop heights are, respectively, $\mathrm{Z_{max}}$ and $\mathrm{Z_{min}}$.
The friction term is integrated, according to Eq. (9). The friction pressure drop, overcome by the buoyancy during the natural circulation, is defined by ΔP_f.
Now, the second left term of Eq. (3) is integrated, according to Eq. (10), where Q is the primary fluid flow rate.

$$\int \left(\frac{G \partial u}{\partial x} \right) dx = \int G \left(\frac{1}{A} \frac{\partial Q}{\partial x} + \frac{Q}{A} \frac{-1}{A} \frac{\partial A}{\partial x} \right) dx = 0 \tag{10}$$

$$\int \rho \left(\frac{\partial u}{\partial t} \right) dx = \int \rho \left(\frac{1}{A} \frac{\partial Q}{\partial t} + \frac{Q}{A} \frac{-1}{A} \frac{\partial A}{\partial t} \right) dx = \frac{\partial Q}{\partial t} \int \left(\frac{\rho}{A} \right) dx \tag{11}$$

$$\frac{dQ}{dt} = \frac{\Delta P_b - \Delta P_f}{\int \left(\frac{\rho}{A} \right) dx} \tag{12}$$

Following the treatment of [4], it is assumed a constant flow rate throughout the loop, that is, $\frac{\partial Q}{\partial x} = 0$. In the NCL case, such assumption is certainly acceptable, since the difference

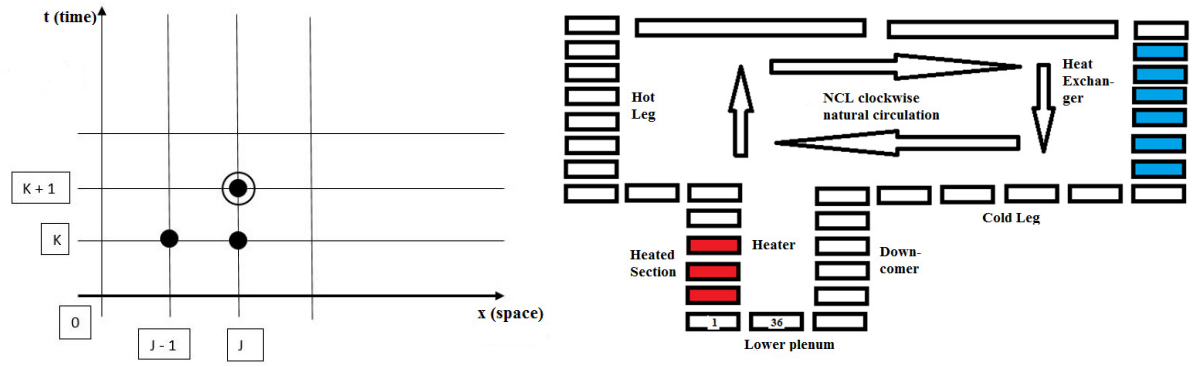

Figure 3: NCL discretization mesh and nodalization.

of flow rates between the hot and the cold leg (using the Boussinesq approximation) is less than 0.35% of the respective nominal value. Finally, the first left term of Eq. (3) is integrated in Eq. (11). Again according to [4], it is assumed that $\frac{\partial Q}{\partial t}$ is constant throughout the loop, regardless of the position x. Using in Eq. (3) the results from Eq. (8) through (11), one gets Eq. (12). It defines the loop flow rate, from the momentum conservation equation.
Now, Eq. (7), together with Eq. (5), as well as Eq. (6) and Eq. (12), are ready to be discretized and then solved as a set of finite difference equations. This will allow for the attainment of the NCL temperatures and flow rate.
The constitutive relation for the density, in Eq. (13), is a conversion, to SI units, of the equation presented in English units by [4].

$$\rho = 0.0000077T^3 - 0.0046T^2 - 0.039T + 1000.45 \tag{13}$$

The inaccuracy of Eq. (13) is less than 0.01% at low pressures and temperatures less than 149 °C, which are the NCL case.

3.2.2. Discretization of the equations

The mathematical model presented above was conveniently discretized, so that a set of finite differences could be solved, instead of the partial differential equations representative of the primary fluid momentum and energy, which are coupled via the flow rate, and consequently much harder to solve.
Fig. 3 shows the NCL discretization mesh and nodalization scheme. The encircled point is the one being calculated, as a function of the others. The algorithm of solution applied to the finite differences set was explicit, marching, as for the temporal discretization of time step Δt, in an upwind scheme, regarding the spatial discretization of node length Δx. As for the nodalization, the loop was split into 36 nodes. The dimensions of the nodes are in Table 1. The term $1/(A\Delta x)$ was included because it appears very often in the NCL discretized equations.
Now, the expansion tank equations will be presented, followed by the primary and secondary fluid temperature equations and the primary flow rate equations.
The air compression in the expansion tank is modelled, in the specific NCL case, by means of an equation of air volume conservation. This is possible because the NCL expansion tank is closed, following similarity with the AP600 PRHR. The air compression by the

Table 1: NCL node dimensions

Node number	Length $L = \Delta x$ (m)	Area A (m^2)	$1/(A\Delta x)$ (m^{-3})
1;35	0.05	0.00718	2786.33
2-6	0.123	0.00581	1398.46
7	0.12	0.00043	459.8
8-15	0.131	0.00043	17696.18
16-17	0.125	0.00043	18603.77
18;25	0.18	0.0296	187.17
19-24	0.1	0.00542	1846.96
26-28	0.15	0.00043	15503.14
29	0.15	0.135	49.38
30-34	0.142	0.00422	1666.85
36	0.064	0.0056	2786.33

dilating primary water, during an experiment, is modelled as an isentropic compression of the air, seen as a perfect gas, so the relation $p.(V_{\text{air}})^{\gamma} = C$ is employed, where p is the air pressure in the expansion tank, V_{air} is its volume, C is a constant, and γ is the specific heat ratio (C_p/C_v), which is assumed 1.4 (air).
Initially, the NCL average temperature $\overline{T}$ is obtained, according to Eq. (14). From now on, the subscript j represents the index of each NCL node, so that the volume of each node is V_j, and N is the total number of NCL nodes.

$$\overline{T} = \frac{\sum_{j=1}^{N} (T_j.V_j)}{\sum_{j=1}^{N} (V_j)} \tag{14}$$

$$\overline{\rho} = 0.0000077\overline{T}^3 - 0.0046\overline{T}^2 - 0.039\overline{T} + 1000.45 \tag{15}$$

$$V_{ncl} = \frac{M}{\overline{\rho}} \tag{16}$$

$$V_{inc} = V_{ncl} - \sum_{j=1}^{N} (V_j) \tag{17}$$

Then, using the constitutive relation for the density, Eq. (13), the average NCL density is calculated, according to Eq. (15). Next, using the fixed primary water mass, M, the instantaneous value of the total primary volume, V_{ncl} can be calculated, according to Eq. (16). Also, the increment of primary water volume, V_{inc} is calculated in Eq. (17).
However, the primary water volume increment in the expansion tank corresponds to an equal air volume decrement, as long as the tank is closed. Then, the air pressure, p, is given by Eq. (18), assuming its compression as an isentropic process. The initial air volume and pressure are, respectively, V_0 and the atmospheric pressure p_{atm}.

$$p = p_{atm} \left(\frac{V_0}{V_0 - V_{inc}} \right)^{1.4} \tag{18}$$

$$T_{sat} = 79.8 + 0.00020445p \tag{19}$$

Moreover, according to the Principle of Pascal, the pressure increase in the expansion tank is transmitted to the primary fluid, which affects the local water saturation temperature

in the nearby heater. The unique situation now described, experimentally observed in the NCL, represents a phenomenon of self-pressurization without self-regulation of the pressure, not found in the previous literature so far. It is called natural circulation under variable pressure (NCVP), according to [11].
The main effect of the NCVP, which is the increase in the local water saturation temperature, is modelled in Eq. (19). It is a linear regression model, in which the the heater exit saturation temperature, T_{sat}, is calculated as a function of the increased primary pressure, p. It is applicable because of the relatively small variations of the involved pressure (less than 150 kPa, absolute) and temperature (less than 112 °C).
The correlation coefficient of the linear regression model above is greater than 99.6%. The saturation temperature increase, on its turn, interferes directly in the NCL geysering phenomenon, as long as it is triggered when the heater exit primary water temperature reaches the local saturation value.
Now, the temperature discretized equations will be presented in a grouped fashion, according to the main NCL components. In the notation employed, in accordance with Fig. 3, $T_{(j,k)}$ stands for the primary fluid temperature T on NCL node j at time k. Such subscripts have the same meaning for the other variables employed in the present work. Eq. (20), (21) and (22) are the discretized forms of the heater temperature equations, applicable to the heating elements, the primary fluid and the the heater walls, respectively.

$$T_{h(j,k+1)} = T_{h(j,k)}\left(1 - \frac{H_h \Delta t}{\rho_h C_{ph} \delta_h}\right) + T_{(j,k)}\left(\frac{H_h \Delta t}{\rho_h C_{ph} \delta_h}\right) + \frac{q'' \Delta t}{\rho_h C_{ph} \delta_h} \tag{20}$$

$$\begin{aligned} T_{(j,k+1)} = \quad & T_{(j,k)}\left(1 - \tfrac{Q\Delta t}{A\Delta x} - \tfrac{H_h P_h \Delta t}{\rho C_p A} - \tfrac{H_w P_w \Delta t}{\rho C_p A}\right) + \\ & T_{(j-1,k)}\left(\tfrac{Q\Delta t}{A\Delta x}\right) + T_{h(j,k)}\left(\tfrac{H_h P_h \Delta t}{\rho C_p A}\right) + T_{w(j,k)}\left(\tfrac{H_w P_w \Delta t}{\rho C_p A}\right) \end{aligned} \tag{21}$$

$$T_{w(j,k+1)} = T_{w(j,k)}\left(1 - \frac{H_w \Delta t}{\rho_w C_{pw} \delta_w}\right) + T_{(j,k)}\left(\frac{H_w \Delta t}{\rho_w C_{pw} \delta_w}\right) \tag{22}$$

Next, the discretized form of the equation for the primary fluid temperature in the NCL pipes is shown in Eq. (23). The equation for the pipe walls (structure) is Eq. (22) above.

$$\begin{aligned} T_{(j,k+1)} = \quad & T_{(j,k)}\left(1 - \tfrac{Q\Delta t}{A\Delta x} - \tfrac{H_w P_w \Delta t}{\rho C_p A}\right) + \\ & T_{(j-1,k)}\left(\tfrac{Q\Delta t}{A\Delta x}\right) + T_{w(j,k)}\left(\tfrac{H_w P_w \Delta t}{\rho C_p A}\right) \end{aligned} \tag{23}$$

Then, the NCL heat exchanger equations, referring to the primary fluid, coolant and structure, respectively, are discretized according to the following Eq. (24), (25) and (26).

$$\begin{aligned} T_{(j,k+1)} = \quad & T_{(j,k)}\left(1 - \tfrac{Q\Delta t}{A\Delta x} - \tfrac{U_1 P_1 \Delta t}{\rho C_p A}\right) + \\ & T_{(j-1,k)}\left(\tfrac{Q\Delta t}{A\Delta x}\right) + T_{c(j,k)}\left(\tfrac{U_1 P_1 \Delta t}{\rho C_p A}\right) \end{aligned} \tag{24}$$

$$\begin{aligned} T_{c(j,k+1)} = \quad & T_{c(j,k)}\left(1 - \tfrac{Q_c \Delta t}{A_c \Delta x_c} - \tfrac{U_2 P_2 \Delta t}{\rho_c C_{pc} A_c} - \tfrac{H_w P_w \Delta t}{\rho_c C_{pc} A_c}\right) + \\ & T_{c(j-1,k)}\left(\tfrac{Q_c \Delta t}{A_c \Delta x_c}\right) + T_{(j,k)}\left(\tfrac{U_2 P_2 \Delta t}{\rho_c C_{pc} A_c}\right) + T_{w(j,k)}\left(\tfrac{H_w P_w \Delta t}{\rho_c C_{pc} A_c}\right) \end{aligned} \tag{25}$$

$$T_{w(j,k+1)} = T_{w(j,k)}\left(1 - \frac{H_w \Delta t}{\rho_w C_{pw} \delta w}\right) + T_{c(j,k)}\left(\frac{H_w \Delta t}{\rho_w C_{pw} \delta_w}\right) \tag{26}$$

Now, the flow rate Eq. (12) is discretized. It is first simplified with the division by the gravity acceleration, g, according to Eq. (27), (28) and (29).

$$\frac{1}{g}\int\left(\frac{\rho}{A}\right)dx = \frac{\rho}{g}\sum_{j=1}^{N}\left(\frac{L_j}{A_j}\right) = a_{\mathrm{l}} \tag{27}$$

$$\frac{1}{g}\Delta P_b = \sum_{j=1}^{N}\left(\rho_j Z_j\right) = H_{\mathrm{l}} \tag{28}$$

$$\frac{1}{g}\Delta P_f = \sum_{j=1}^{N}\frac{\rho f_{\mathrm{j}} {u_{\mathrm{j}}}^2 L_{\mathrm{j}}}{2D_{e\mathrm{j}}g} = \frac{\rho Q^2}{2g}\sum_{j=1}^{N}\frac{f_{\mathrm{j}}.L_{\mathrm{j}}}{D_{e\mathrm{j}}{A_{\mathrm{j}}}^2} \tag{29}$$

Eq. (27) and (28) introduce, respectively, the loop constant a_{l}, which depends only on the loop geometry, and the hydraulic head H_{l}, as defined by [4]. Similarly, Eq. (30) defines the total loop resistance R_{l}, already with the form loss term K_{j} added to the friction term. Finally, Eq. (31) allows for the calculation of the NCL flow rate temporal variation and Eq. (32) is the discretized form of the loop flow rate equation.

$$R_{\mathrm{l}} = \frac{\rho Q^2}{2g}\sum_{j=1}^{N}\frac{1}{{A_{\mathrm{j}}}^2}\left(\frac{f_{\mathrm{j}}L_{\mathrm{j}}}{D_{e\mathrm{j}}} + K_{\mathrm{j}}\right) \tag{30}$$

$$\frac{dQ}{dt} = \frac{H_{\mathrm{l}} - R_{\mathrm{l}}}{a_{\mathrm{l}}} \tag{31}$$

$$Q_{(\mathrm{k}+1)} = Q_{(\mathrm{k})} + \frac{\Delta t}{a_{\mathrm{l}}}\left(H_{\mathrm{l}(\mathrm{k}+1)} - R_{\mathrm{l}(\mathrm{k})}\right) \tag{32}$$

3.2.3. NCL computational modelling

The computational program, originated in the equations presented in the previous section, was implemented in MATLAB. The algorithm employed, after the initialization of the variables, calculates the different NCL temperatures for the next time step. Then, the densities of all NCL nodes are calculated. Next, the buoyancy and the friction terms are calculated. Finally, the loop flow rate is obtained. After all these steps, the simulation time is incremented. The program is ended when the simulation time reaches the high value, of the order of 30000 to 40000 s, typical of the long NCL transient [11].
Because an explicit algorithm is used, its stability condition must be pointed out. The corresponding analysis was carried out following [14]. Eq. (33) shows the stability condition, based on the Courant number, C, no greater than unity.

$$C = \left(\frac{Q}{A}\right)\frac{\Delta t}{\Delta x} \leq 1 \tag{33}$$

4. RESULTS AND DISCUSSIONS

All results shown in this section were obtained in NCL experiments, with the heating power of 1030 W and a coolant flow rate with one of the following values: 3 l/h, 6 l/h, 9 l/h or 12 l/h. The experiments took a total time between 30000 and 40000 s, being terminated

only after the two-phase flow was observed in the form of geysering eruptions. In this way, the experiments with the maximum coolant flow rate, of 12 l/h, were the longest. For more details about the NCL experiments, the two-phase flow patterns observed and respective snapshots, see [11].
The variables used in the comparison between experimental and calculated data, via the MATLAB model implemented, as above mentioned, were some relevant loop temperatures and pressures, as shown in the next two subsections.

4.1. Temperatures

In the MATLAB model validation against the NCL experimental data, the temperatures compared were the heater exit temperature (highest primary water temperature), and the HX exit coolant temperature (highest secondary water temperature).
The heater exit temperature is very important in the NCL case, since it triggers the geysering occurrence, when it reaches the local water saturation value. On its turn, the saturation temperature is directly influenced by the specific NCL condition of NCVP. In this way, the modeled saturation temperature is also presented in the results, as it should function as an external envelope, maximum value for the heater exit temperature. Finally, the coolant temperature in the HX exit is important because it permits the evaluation of the heat exchanging modelling, with a constant coolant inlet temperature of 25 °C.
The next graphs show the primary fluid temperatures, at the heater exit, and its modelled saturation limit, as well as the coolant temperature, at the HX exit, with the coolant flow rates of 3, 6, 9 and 12 l/h, according to Fig. (4).
By examining these graphs, one observes that, in general, there was reasonable agreement between the experimental and the calculated temperatures, especially at lower temperatures, in the single-phase flow, to which the present modelling is oriented.
The heater exit experimental and modelled temperatures were closer than the corresponding HX exit values. This may be improved by changing the correlations used for obtaining the HX internal and external global heat transfer coefficients.
For all cooling rates, the saturation limit temperature, modelled from the NCVP formulation, functioned well, as an envelope (superior) limit for the heater exit temperature. Moreover, the modelled saturation limit and heater exit curves had a point of intersection in the presented time window, for all graphs. Such point represents the modelled first geysering occurrence, when the heater exit temperature reaches the local water saturation value. In the experimental heater exit curve, on the other hand, the first geysering occurrence is indicated by the first peak, maximum heater exit temperature. The first geysering experimental times were, approximately: 19000 s, for the cooling rate of 3 l/h ; 20000 s, for 6 l/h; 23000 s, for 9 l/h; 32000 s, for 12 l/h.

4.2. Pressures

In the present model evaluation, by a comparison to the NCL experimental data, the absolute pressures compared - experimental and calculated - refer to the location just below the heater upper cover. Such NCL pressure sensor positioning was chosen for confirming that geysering, and not the natural circulation oscillation, was the instability type occurring in the loop, in the beginning of two-phase flow, as seen in [11].
Moreover, the pressure measurement described above served as the experimental confir-

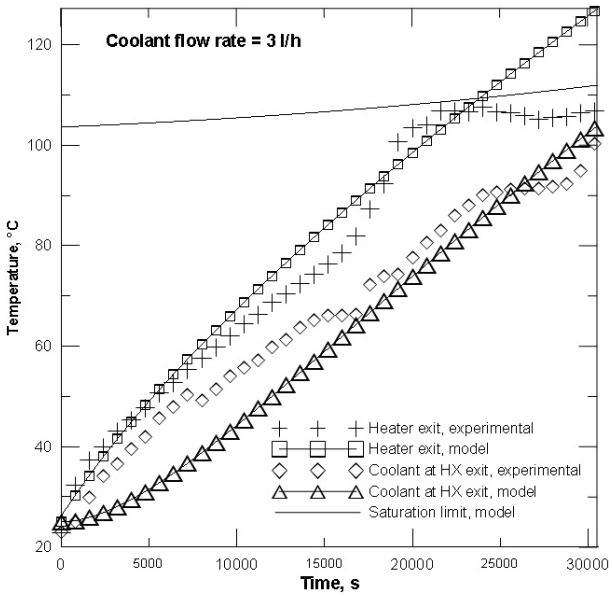

(a) Coolant flow rate 3 l/h

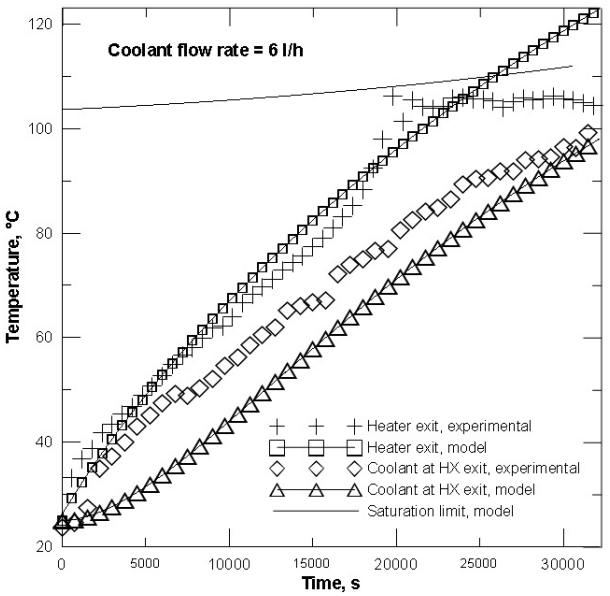

(b) Coolant flow rate 6 l/h

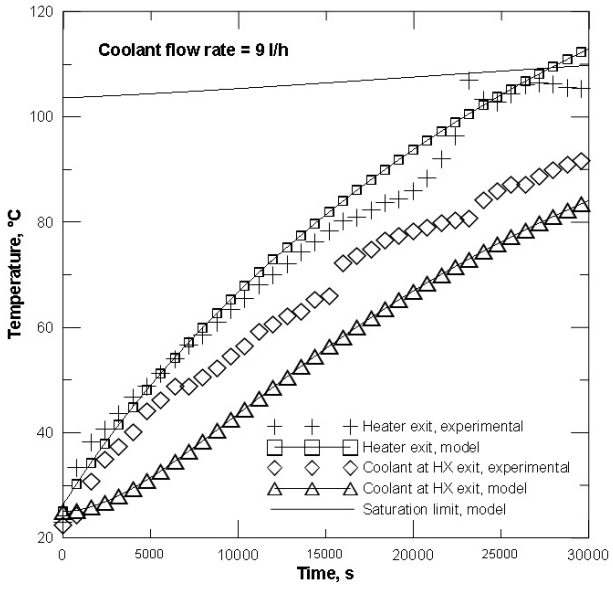

(c) Coolant flow rate 9 l/h

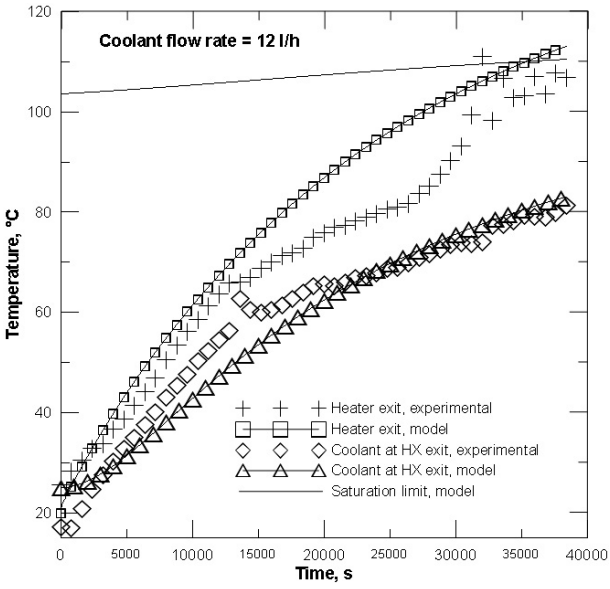

(d) Coolant flow rate 12 l/h

Figure 4: Comparison between experimental and modelled NCL temperatures.

mation of the proposed NCVP explanation for the NCL behavior. According to it, an abrupt pressure increase should be observed in the NCL primary pressure, during the primary water heating characteristic of an experiment, because of the proximity between the expansion tank - where the pressure increase was originated, by an isentropic compression of its residual air - and the heater, to where the pressure was transmitted, in accordance with the Principle of Pascal.
Fig. (5) shows the experimental and calculated NCL absolute pressure values below the heater upper cover, with coolant flow rates of 3, 6, 9 and 12 l/h.
The pressure graphs show that the experimental NCL pressures, below the heater upper cover, confirm the NCVP explanation proposed for the NCL, as long as an exponential pressure increase is observed before the maximum pressure is achieved. On its turn, this happens simultaneously with the first geysering occurrence, as detailed in [11].
The calculated pressures agree qualitatively with the experimental data. The modelled curves show an increasing behavior before the maximum pressure point, like the experimental curves. However, the rate of pressure increase differs between the curves, what is attributed to the beginning of vapor formation in the NCL, well before the first geysering. The reason here is that the modelled curve is totally based on the calculation of the NCL total primary fluid volume, which was carried out assuming single-phase only. The bubble formation in the loop, even from its very beginning, much time before the geysering occurrence, totally distorts such volume calculation, in an exponential fashion.

5. CONCLUSIONS

In the present work, a model, initially oriented to the single-phase flow, was elaborated in order to study the transient behavior of a natural circulation loop, and the results thus obtained agreed qualitatively well with the experimental data.
The loop, named NCL, was built following similarity criteria to the AP600 PRHR system, in a 1:10 scale in height. A long transient characterized its operation, which occurred mostly in single-phase flow. A condition of self-pressurization without self-regulation of the pressure, not seen in the previous literature so far, was experimentally observed, and named NCVP, natural circulation under variable pressure.
A classical model was used as a starting point for the study. However, several improvements were added in the present modelling. These improvements included the consideration of the different thermal capacities of the heating elements and the heater walls; the coolant heating during the heat exchanging process, in the heat exchanger; the addition of the form pressure loss to the friction term, in the momentum conservation equation; and the NCL self-pressurization, which originates the NCVP, modelled as an isentropic compression of a perfect gas, that is, the air in the expansion tank, with transmission to the primary fluid in the heater via the Principle of Pascal.
A set of finite difference equations was implemented in a MATLAB program, in order to produce the results of the modelling. Such results were compared to the corresponding NCL experimental data, for evaluating the model. In the case of the temperatures, a better agreement was obtained for the lower values, during the single-phase flow, to which the present model was oriented. In the case of the pressures, it was more difficult to obtain agreement between calculated and experimental data. Such difficulty arose because the NVCP pressure calculation was entirely based on the variation of the loop single-phase primary volume. So, the presence of bubbles in the primary fluid, much time before the

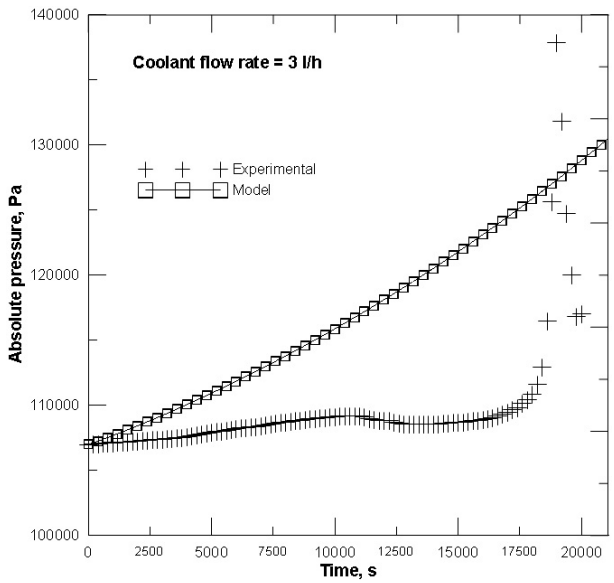

(a) Coolant flow rate 3 l/h

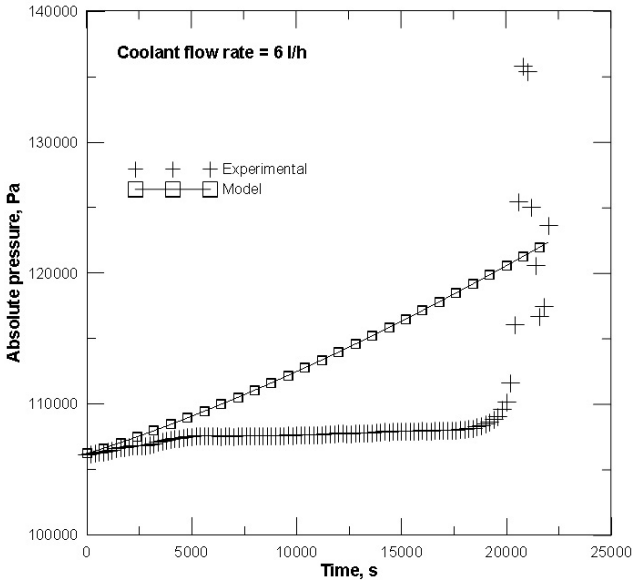

(b) Coolant flow rate 6 l/h

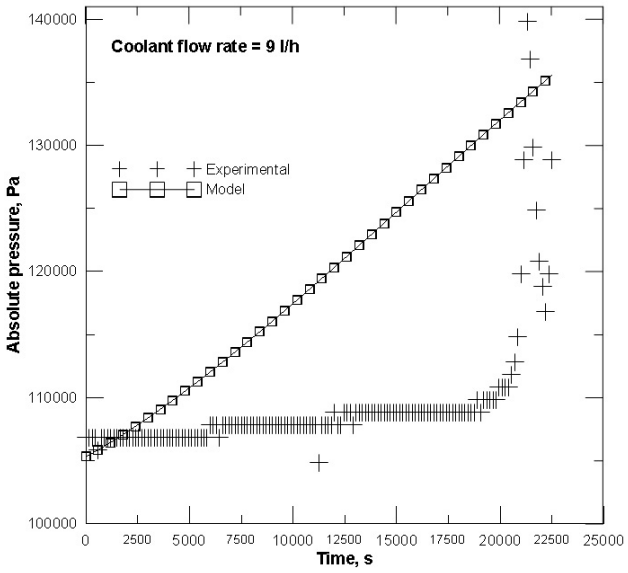

(c) Coolant flow rate 9 l/h

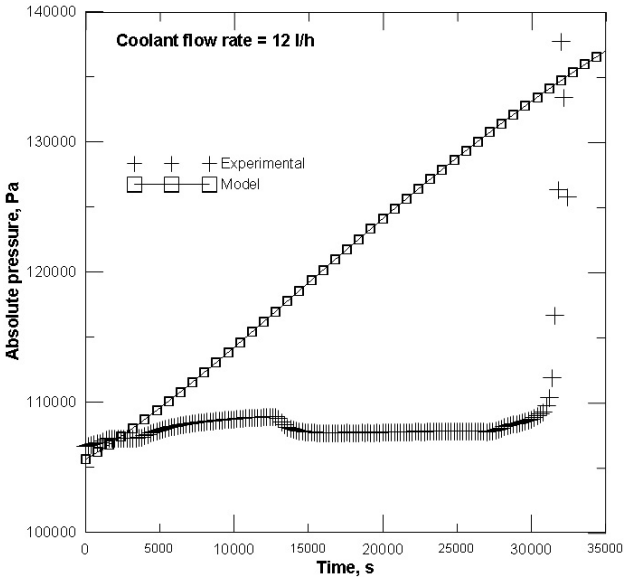

(d) Coolant flow rate 12 l/h

Figure 5: Comparison between experimental and modelled NCL pressure below the heater upper cover.

first geysering, distorted the volume calculation, in an exponential fashion, because of the isentropic compression process, thus distorting the pressure calculation, too.
In this way, both temperature and pressure results got from the present model, oriented to single-phase flow, indicated the necessity of including, in the transient NCL analysis, the two-phase flow modelling, currently planned as a future research work.

ACKNOWLEDGMENTS

The authors acknowledge the financial support by CNPq and FAPERJ.

REFERENCES

1. D. W. Murphy, "An Experimental Investigation of Geysering in Vertical Tubes", *Advanced Cryogenics Engineering*, **10**, pp. 353–359, (1965).
2. V. K. Chexal and A. E. Bergles, "Two-Phase Instabilities in a Low Pressure Natural Circulation Loop", *AIChE Symposium Series*, **69**, pp. 37–45, (1973).
3. Y. F. Rao, K. Fukuda and T. Koga, "Experimental and Numerical Study of Two-Phase Flow Instabilities in Natural-Circulation Boiling Channels", 5^{th} *International Conference on Nuclear Engineering*, Nice, France, May 26-30, (1997).
4. C. D. Alstad, H. S. Isbin, N. R. Amundson *et al.*, "Transient Behavior of Single-Phase Natural-Circulation Loop Systems", *AIChE Journal*, **1**, pp. 417–425, (1955).
5. E. H. Wissler, H. S. Isbin and N. R. Amundson, "Oscillatory Behavior of a Two-Phase Natural-Circulation Loop", *AIChE Journal*, **2**, pp. 157–162, (1956).
6. Y. Zvirin, P. R. Jeuck III, C. W. Sullivan *et al.*, "Experimental and Analytical Investigation of a Natural Circulation System with Parallel Loops", *Journal of Heat Transfer*, **103**, pp. 645–652, (1981).
7. J. Gou, S. Qiu, G. Su *et al.*, "Thermal Hydraulic Analysis of a PRHR System for an Integral PWR", *Sc. and Tech. of Nuc. Ins.*, **2009**, Art. ID 473795, 12 pp., (2009).
8. F. D'Auria and G. M. Galassi, "Flowrate and Density Oscillations during Two-Phase Natural Circulation in PWR", *Nuc. Eng. and Des.*, **122**, pp. 209-218, (1990).
9. K. Naveen, K. N. Iyer, J. B. Doshi *et al.*, "Investigations on Single-Phase Natural Circulation Loop Dynamics. Part 3: Role of Expansion Tank", *Progress in Nuclear Energy*, **78**, pp. 65-79, (2015).
10. P. Zanocco, M. Giménez and D. Delmastro, "Modeling Aspects in Linear Stability Analysis of a Self-Pressurized, Natural Circulation Integral Reactor ", *Nuc. Eng. and Des.*, **231**, pp. 283-301, (2004).
11. A. L. B. Vianna, J. L. H. Faccini and J. Su "Experimental Study of Two-Phase Flow Oscillations in a Natural Circulation Loop", http://www.sistema.abcm.org.br/articleFiles/download/1461, 16^{th} *Braz. Congress of Thermal Sc. and Eng.*, Vitória, ES, Brazil, November 07-10, (2016).
12. N. E. Todreas and M. S. Kazimi. *Nuclear Systems I*, Taylor & Francis, (1993).
13. N. E. Todreas and M. S. Kazimi. *Nuclear Systems II*, Taylor & Francis, (2001).
14. D. A. Anderson, J. C. Tannehill and R. H. Pletcher. *Computational Fluid Mechanics and Heat Transfer*, Hemisphere Publishing, (1984).